INTERNATIONAL JOURNAL FOR NUMERICAL METHODS IN FLUIDS
Int. J. Numer. Meth. Fluids 2008; **56**:1321–1328
Published online 27 December 2007 in Wiley InterScience (www.interscience.wiley.com). DOI: 10.1002/fld.1712

Variants of projection-based finite element variational multiscale methods for the simulation of turbulent flows

Volker John and Adela Kindl*,†

FR 6.1-Mathematik, Universität des Saarlandes, Postfach 15 11 50, 66041 Saarbrücken, Germany

SUMMARY

Some variants of a three-scale projection-based finite element variational multiscale (VMS) method are studied for turbulent channel flow computations at $Re_\tau = 180$. Different spaces for the large scales, two eddy viscosity models and two ways of discretizing the projection terms in time are explored. The results obtained with the resolved small scales in the definition of the eddy viscosity are very sensitive to the temporal discretization of the projection terms. The computations were performed on three grids commonly used in turbulent channel flow simulations. Copyright © 2007 John Wiley & Sons, Ltd.

Received 11 April 2007; Revised 7 November 2007; Accepted 7 November 2007

KEY WORDS: VMS methods; finite element methods; turbulent channel flow

1. INTRODUCTION

Variational multiscale (VMS) methods are a rather new approach for simulating turbulent flows. They are based on basic ideas from [1, 2] and the first application of these ideas to turbulent flow simulations can be found in [3]. Meanwhile, different classes and realizations of VMS methods exist, e.g. see [4–9]. The main feature of VMS methods is the definition of scales by projections into function spaces. Naturally, scales smaller than the mesh width, the unresolved scales, cannot be computed. A first class of VMS methods uses a two-scale decomposition of the flow and multiscale concepts are applied to model the influence of the unresolved scales onto the resolved ones [9]. A second class is based on a three-scale decomposition, where the resolved scales are decomposed into large and small ones [8]. It is assumed that the scale separation is performed

*Correspondence to: Adela Kindl, FR 6.1-Mathematik, Universität des Saarlandes, Postfach 15 11 50, 66041 Saarbrücken, Germany.
†E-mail: adela@c-kindl.de

Contract/grant sponsor: Deutsche Forschungsgemeinschaft (DFG); contract/grant number: Jo 329/7-1

such that the direct influence of the unresolved scales onto the large scales can be neglected. The impact of the unresolved scales onto the resolved small scales is modeled by an eddy viscosity model. The definition of the scales by projections and the ways of taking the effect of the subgrid scales into account are important differences to classical LES methods, see [10] for a detailed discussion, and they avoid problems like commutation errors on boundaries [11, 12].

This paper considers a three-scale VMS method in the context of finite element discretizations, the so-called projection-based VMS method, described in Section 2. Recently, an assessment of this method for the benchmark problem of the turbulent channel flow at $Re_\tau = 180$ has been started [10]. The present paper will continue these investigations and study in particular some variants of this VMS method with respect to the definition of the eddy viscosity model and the discretization of the projection terms in time.

2. PROJECTION-BASED THREE-SCALE FINITE ELEMENT VMS METHODS

Let $V^h \times Q^h$ be a pair of inf–sup stable, conforming finite element spaces for velocity and pressure. In addition, let L^H be a finite dimensional space of symmetric $d \times d$ tensor-valued functions representing a large-scale space, and a non-negative function ν_T acting as the turbulent viscosity. The semi-discrete three-scale projection-based VMS method with parameters ν_T and L^H then seeks $\mathbf{u}^h : [0,T] \to V^h$, $p^h : (0,T] \to Q^h$, and $\mathbb{G}^H : [0,T] \to L^H$ such that

$$\begin{aligned}
&(\mathbf{u}_t^h, \mathbf{v}^h) + (2\nu\mathbb{D}(\mathbf{u}^h), \mathbb{D}(\mathbf{v}^h)) + ((\mathbf{u}^h \cdot \nabla)\mathbf{u}^h, \mathbf{v}^h) \\
&\quad -(p^h, \nabla\cdot\mathbf{v}^h) + (\nu_T(\mathbb{D}(\mathbf{u}^h) - \mathbb{G}^H), \mathbb{D}(\mathbf{v}^h)) = (\mathbf{f}, \mathbf{v}^h) \quad \forall \mathbf{v}^h \in V^h \\
&\qquad (q^h, \nabla\cdot\mathbf{u}^h) = 0 \quad \forall q^h \in Q^h \\
&\qquad (\mathbb{D}(\mathbf{u}^h) - \mathbb{G}^H, \mathbb{L}^H) = 0 \quad \forall \mathbb{L}^H \in L^H
\end{aligned} \tag{1}$$

The last equation in (1) states that $\mathbb{G}^H$ is the L^2-projection of $\mathbb{D}(\mathbf{u}^h)$ into L^H. Thus, $\mathbb{G}^H$ represents large scales of $\mathbb{D}(\mathbf{u}^h)$ and, consequently, $\mathbb{D}(\mathbf{u}^h) - \mathbb{G}^H$ represents resolved small scales. Hence, the additional term $(\nu_T(\mathbb{D}(\mathbf{u}^h) - \mathbb{G}^H), \mathbb{D}(\mathbf{v}^h))$, introduced by three-scale VMS methods, is a viscous term acting directly only on the resolved small scales.

Two static Smagorinsky-type eddy viscosity models for the turbulent viscosity will be considered in the numerical tests:

- using all resolved scales: $\nu_T = C_S\delta^2 \|\mathbb{D}(\mathbf{u}^h)\|_F$,
- using only the resolved small scales: $\nu_T = C_S\delta^2 \|\mathbb{D}(\mathbf{u}^h) - \mathbb{G}^H\|_\mathrm{F}$,

where $\|\cdot\|_\mathrm{F}$ is the Frobenius norm. Smagorinsky-type models are commonly used as turbulence models in three-scale VMS methods. Numerical studies show that using the static Smagorinsky model within VMS methods works well, often not worse than the dynamic Smagorinsky model, sometimes even better [7, 13].

All terms of (1) that occur in the Galerkin finite element formulation of the Navier–Stokes equations will be treated implicitly in time. The L^2-projection for the definition of $\mathbb{G}^H$ will be treated explicitly as well as implicitly. The implicit discretization is described in detail in [8].

DOI: 10.1002/fld

Its main features are:

- it is only efficient if L^H is a discontinuous finite element space on the finest grid and the basis of L^H is chosen to be L^2-orthogonal,
- seven sparse matrices whose dimensions depend on V^h and L^H are needed,
- four of these matrices have to be assembled only once at the initial time,
- the three other matrices have to be assembled at each discrete time in each step of the iteration for solving the nonlinearity, since they depend on ν_T and ν_T depends on the current finite element solution,
- matrix–matrix products have to be computed at each discrete time in each step of the iteration for solving the nonlinearity.

The explicit discretization of the projection term in the additional viscous term removes the restriction on L^H [14]. It is also somewhat cheaper than the implicit approach. Instead of the costs given in the last two points, the following arise [15]:

- the three other matrices have to be assembled only once at each discrete time,
- matrix–vector products have to be computed only once at each discrete time.

Note that the assembling of matrices in three-dimensional computations is quite expensive [16]. Altogether, one can expect faster computations with the explicit approach. The amount of speed-up will be studied in the numerical tests.

3. NUMERICAL RESULTS FOR THE TURBULENT CHANNEL FLOW AT $Re_\tau = 180$

The definition of the turbulent channel flow problem at $Re_\tau = 180$ as well as references can be found in [17]. Its setup and the computation of the values of interest in our simulations have been discussed in detail in [10]. Starting with an already developed flow field, each solution was allowed to develop further for 10 s (dimensionless) and statistics were computed for another 20 s.

The computations were performed with the code *MooNMD* [18]. Hexahedral grids with $V^h \times Q_h = Q_2 \times P_1^{\text{disc}}$ were used, i.e. the pressure finite elements are piecewise linear and discontinuous. For the temporal discretization, the Crank–Nicolson scheme was used with the equidistant time steps $\Delta t = 0.002$ and 0.004. Both time steps are smaller than the Kolmogorov time scale and they fit into the range of time steps proposed in [19]. The following variants of the projection-based VMS method will be studied:

- $L^H \in \{P_0, P_1^{\text{disc}}\}$; abbreviations: VMS0, VMS1;
- explicit and implicit temporal discretization of the projection term in the momentum equation and the L^2-projection, abbreviations: EXPL, IMPL;
- definition of the turbulent viscosity with all resolved scales or only with the resolved small scales, abbreviations: ALL, SMALL.

In [8, 10], only VMS0_IMPL_ALL and VMS1_IMPL_ALL were considered.

The computations were performed on grids that are uniform in streamwise and spanwise direction but which become finer toward the walls in the wall-normal direction. We studied three different types of the distribution of the grid points in wall-normal direction, $i = 0, \ldots, N_y$, where N_y is the

DOI: 10.1002/fld

number of grid points:

- Grid 1: $y_i = 1-\cos(i\pi/N_y)$, $y^+_{\min} = 1.7293$, [7, 10];
- Grid 2: $y_i = 1+\tanh(2.75(2i/N_y-1))/\tanh(2.75)$, $y^+_{\min} = 0.7244$, [10, 19];
- Grid 3: $y_i = 1+\tanh(2(2i/N_y-1))/\tanh(2)$, $y^+_{\min} = 2.115$, [6].

Grid 2 of the present study is the same as Grid 0 from [10]. The degrees of freedom (d.o.f.), which are not located on mesh cell boundaries in the wall-normal direction, do not obey the prescribed distribution but are located as it is usual in finite element methods, i.e. in the center between the mesh cell boundaries for the Q_2 finite element. The number $y^+_{\min}$ is the smallest distance of a velocity d.o.f. to the wall, measured in wall units $y^+ = Re_\tau y$. The numerical studies were performed on $8\times 16\times 8$ grids, which results in 25 344 velocity d.o.f. (including Dirichlet nodes) and 4096 pressure d.o.f. These coarse grids require the application of a turbulence model since a direct numerical simulation (DNS) blows up in a finite time [10]. The dimensions of each component of the large-scale spaces are 1024 for $L^H = P_0$ and 4096 for $L^H = P_1^{\text{disc}}$. The parameter δ in the Smagorinsky models was set to twice the length of the shortest edge of the mesh cells. This is the same choice as in [10] (where, however, in [10] erroneously only once the length of the shortest edge was given).

Two situations for the application of turbulence models can be distinguished:

- the grid is too coarse to allow a DNS, the turbulence model is needed to perform any simulations at all,
- the grid is fine enough to perform an underresolved DNS, the turbulence model is used to improve the results.

The first situation is given if the Reynolds number is very large compared with the grid size. This situation is more common in applications and it is considered here.

We studied the mean velocity profile, the rms turbulence intensities $u^{h,*}_{\text{rms}}$, $v^{h,*}_{\text{rms}}$, $w^{h,*}_{\text{rms}}$ and the off-diagonal Reynolds stress component $\mathbb{R}^{h,*}_{12}$. Qualitatively the same results were obtained for both time steps and we present results for the smaller one.

Representative examples comparing the implicit and explicit discretization of the projection terms are given in Figure 1. Whereas the differences in the curves are small for the turbulent viscosity defined with all resolved scales, the curves obtained with the combination EXPL_SMALL differ considerably from their implicit counterparts. This behavior is caused by the strong fluctuations of the resolved small scales: it makes a big difference if these scales are taken from the previous or the present discrete time. This high sensitivity of the projection terms on the temporal discretization is not desirable. We will consider below only the implicit approach.

Differences from the mean velocity profile for all variants of the implicit approach are shown in Figure 2. The deviation from the reference curve is in general smaller for $C_s = 0.01$ and the results on Grid 1 are better than on the other grids. The curves obtained with the two models for v_T are in general similar.

Results for second-order statistics are given in Figure 3. All simulations overpredict the (absolute) values of the reference curves. The rather large differences to the reference curves are caused by the used coarse grid. We checked that the differences become smaller on finer grids (which allow to perform an underresolved DNS). The overprediction is often smaller for v_T defined with all resolved scales, if all other parameters of the simulations were chosen to be the same. The results obtained with $C_s = 0.01$ are in general closer to the reference curves than the results with

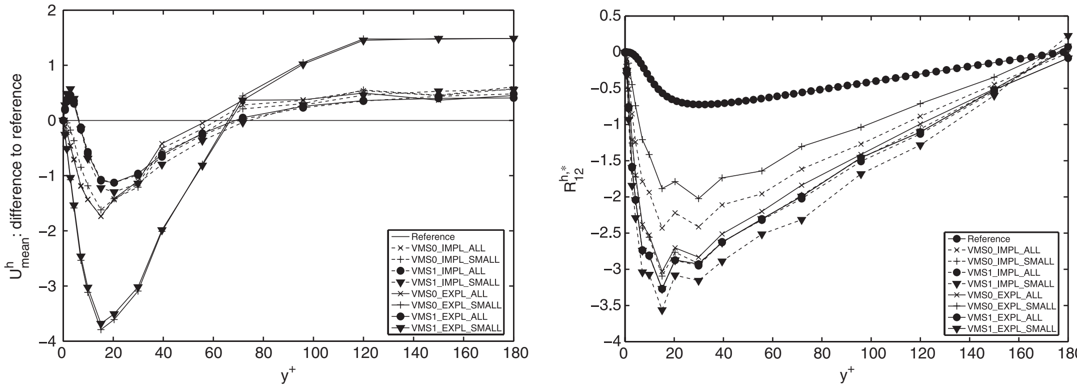

Figure 1. Comparison of the implicit and explicit discretization of the projection terms; left: difference from the mean velocity profile ($U_{\max}=18.301$ at $y^+=180$), Grid 1, $C_s=0.01$ and right: $\mathbb{R}^{h,*}_{12}$, Grid 2, $C_s=0.005$.

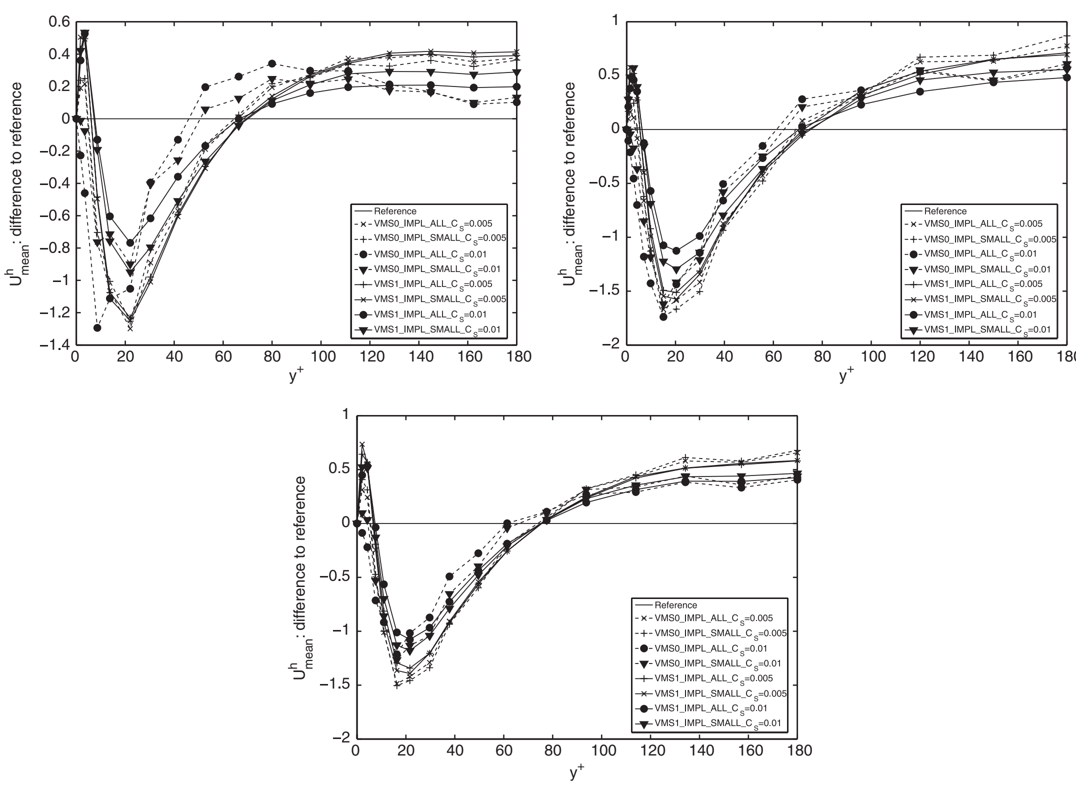

Figure 2. Differences from the reference mean velocity profile ($U_{\max}=18.301$ at $y^+=180$), Grid 1 (left), Grid 2 (right), and Grid 3 (bottom).

DOI: 10.1002/fld

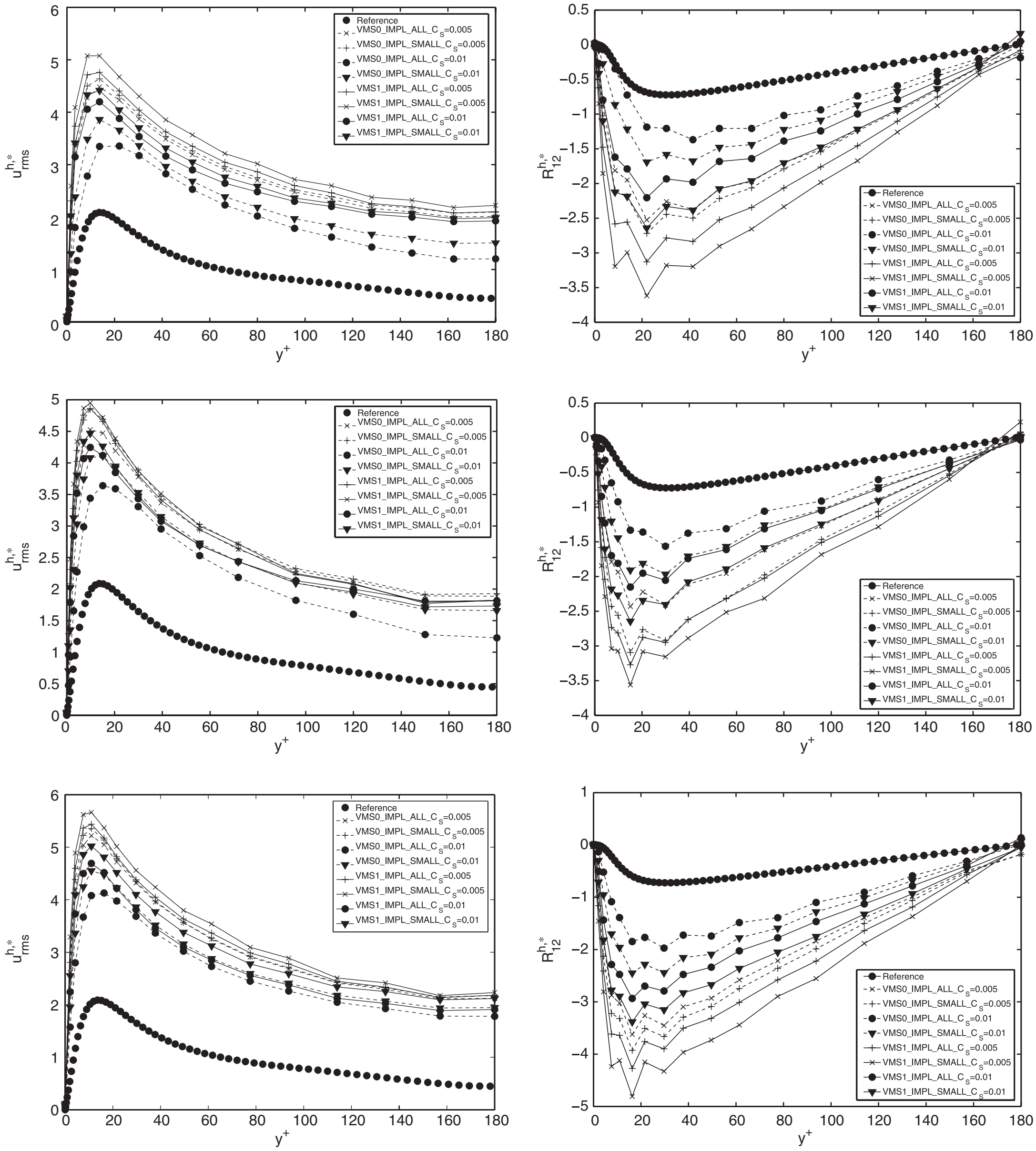

Figure 3. Second-order statistics: $u_{\mathrm{rms}}^{h,*}$ (left), $\mathbb{R}_{12}^{h,*}$ (right); Grid 1, Grid 2, Grid 3 (top to bottom).

$C_s = 0.005$ and VMS0 leads often to better results than VMS1. Thus, the VMS method, which introduces most turbulent viscosity, VMS0_ALL with $C_s = 0.01$, shows the smallest overprediction of the second-order statistics. Comparing the grids, the worst results are always obtained on Grid 3.

DOI: 10.1002/fld

Table I. Computing times in seconds on Grid 1 for a period of 10 s (5000 time steps).

	IMPL_ALL	IMPL_SMALL	EXPL_ALL	EXPL_SMALL
VMS0, $C_s = 0.005$	309 394	315 292	286 341	277 900
VMS1, $C_s = 0.005$	363 972	384 424	340 980	294 674
VMS0, $C_s = 0.01$	228 071	269 520	217 644	203 413
VMS1, $C_s = 0.01$	316 117	333 937	288 845	208 472

Computing times on Grid 1 are given in Table I. The same solver as in [10] was used. For using all resolved scales in the definition of ν_T, the explicit approach saved consistently 5–9% of the computing time compared with the implicit one. The larger differences in the results of both temporal discretizations for the resolved small scales in the definition of ν_T are reflected by larger differences in the computing times. We consider the results with IMPL_SMALL more reliable than with EXPL_SMALL, which is supported for instance with the left picture of Figure 1. The computations with IMPL_SMALL took somewhat more time than the implicit approach with all resolved scales in the definition of ν_T.

4. SUMMARY

This paper investigated variations of parameters in a three-scale projection-based finite element VMS method with respect to the large-scale space, the form of the turbulent viscosity and the temporal discretization of the projection terms. Three different grids commonly used in turbulent flow computations were studied. The computations were performed on rather coarse grids.

The main observation was that the results obtained with the resolved small scales in the definition of ν_T are sensitive to the temporal discretization of the projection terms. Using these scales from different times may led to much different results because of their strong fluctuations. The second-order statistics were overpredicted in all simulations. The method that introduces most viscosity (VMS0_ALL with $C_s = 0.01$) often gave the best results. The results on Grid 3 are often worse than on the other grids. The explicit approach with all resolved scales in ν_T was somewhat (always less than 10%) faster than the corresponding implicit approach.

ACKNOWLEDGEMENTS

The research of A. Kindl was supported by the Deutsche Forschungsgemeinschaft (DFG) by grant No. Jo 329/7-1.

REFERENCES

1. Hughes TJR. Multiscale phenomena: Green's functions, the Dirichlet-to-Neumann formulation, subgrid-scale models, bubbles and the origin of stabilized methods. *Computer Methods in Applied Mechanics and Engineering* 1995; **127**:387–401.
2. Guermond J-L. Stabilization of Galerkin approximations of transport equations by subgrid modeling. *ESAIM: Mathematical Modelling and Numerical Analysis* 1999; **33**:1293–1316.
3. Hughes TJ, Mazzei L, Jansen KE. Large eddy simulation and the variational multiscale method. *Computing and Visualization in Science* 2000; **3**:47–59.

4. Hughes TJR, Oberai AA, Mazzei L. Large eddy simulation of turbulent channel flows by the variational multiscale method. *Physics of Fluids* 2001; **13**:1784–1799.
5. Gravemeier V, Wall WA, Ramm E. A three-level finite element method for the instationary incompressible Navier–Stokes equation. *Computer Methods in Applied Mechanics and Engineering* 2004; **193**:1323–1366.
6. Ramakrishnan S, Collis SS. Multiscale modeling for turbulence simulation in complex geometries. *AIAA Paper 2004–0241*, 2004.
7. Gravemeier V. Scale-separating operators for variational multiscale large eddy simulation of turbulent flows. *Journal of Computational Physics* 2006; **212**:400–435.
8. John V, Kaya S. A finite element variational multiscale method for the Navier–Stokes equations. *SIAM Journal on Scientific Computing* 2005; **26**:1485–1503.
9. Bazilevs Y, Calo VM, Cottrell JA, Hughes TJR, Reali A, Scovazzi G. Variational multiscale residual-based turbulence modeling for large eddy simulation of incompressible flows. *Technical Report*, University of Texas at Austin, ICES, 2007.
10. John V, Roland M. Simulations of the turbulent channel flow at $Re_\tau = 180$ with projection-based finite element variational multiscale methods. *International Journal for Numerical Methods in Fluids* 2007; **55**:407–429.
11. Dunca A, John V, Layton WJ. The commutation error of the space averaged Navier–Stokes equations on a bounded domain. In *Contributions to Current Challenges in Mathematical Fluid Mechanics*, Heywood JG, Galdi GP, Rannacher R (eds). Birkhäuser: Basel, 2004; 53–78.
12. Berselli LC, John V. Asymptotic behavior of commutation errors and the divergence of the Reynolds stress tensor near the wall in the turbulent channel flow. *Mathematical Methods in the Applied Sciences* 2006; **29**:1709–1719.
13. Holmen J, Hughes TJR, Oberai AA, Wells GN. Sensitivity of the scale partition for variational multiscale large-eddy simulation of channel flow. *Physics of Fluids* 2004; **16**:824–827.
14. John V, Kaya S, Layton W. A two-level variational multiscale method for convection-dominated convection–diffusion equations. *Computer Methods in Applied Mechanics and Engineering* 2006; **195**:4594–4603.
15. John V, Tambulea A. On finite element variational multiscale methods for incompressible turbulent flows. *Proceedings of ECCOMAS CFD 2006*, 2006. On CD-ROM, ISBN 90-9020970-0.
16. John V. On the efficiency of linearization schemes and coupled multigrid methods in the simulation of a 3d flow around a cylinder. *International Journal for Numerical Methods in Fluids* 2006; **50**:845–862.
17. Moser DR, Kim J, Mansour NN. Direct numerical simulation of turbulent channel flow up to $Re_\tau = 590$. *Physics of Fluids* 1999; **11**:943–945.
18. John V, Matthies G. MooNMD—a program package based on mapped finite element methods. *Computing and Visualization in Science* 2004; **6**:163–170.
19. Choi H, Moin P. Effects of the computational time step on numerical solutions of turbulent flow. *Journal of Computational Physics* 1994; **113**:1–4.

DOI: 10.1002/fld